Journal of
NANOSTRUCTURES
JNS
NANOSTRUCTURES
JNS.kashanu.ac.ir

Study of Non-Isothermal Crystallization Kinetics of Biodegradable Poly(ethylene adipate)/SiO_2 Nanocomposites

M. R. Memarzadeh[a*], M. Mohsen-Nia[b, c]

[a]*Department of Chemistry, University of Kashan, Kashan, Iran*
[b]*Institute of Nanoscience and Nanotechnology, University of Kashan, Kashan, Iran*
[c]*Department of Engineering, University of Kashan, Kashan, Iran*

Article history:
Received 11/9/2013
Accepted 26/11/2013
Published online 1/12/2013

Keywords:
Nanocomposite
Non-isothermal crystallization
Activation energy
Silica

**Corresponding author:*
E-mail address:
m.r.memarzadeh63@gmail.com
Phone: +983615912376
Fax: +983615912397

Abstract

Poly(ethylene adipte) and poly(ethylene adipate)/silica nanocomposite (PEAd/SiO_2) containing 3 wt. % SiO_2 were prepared by an in situ method. The examinations on the non-isothermal crystallization kinetic behavior have been conducted by means of differential scanning calorimeter (DSC). The Avrami, Ozawa, and combined Avrami and Ozawa equations were applied to describe the crystallization kinetics and to determine the crystallization parameters of the prepared PEAd/SiO_2 nanocomposites. It is found that the inclusion of the silica nanoparticles can accelerate the nucleation rate due to heterogeneous nucleation effect of silica on the polymer matrix. According to the obtained results, the combined Avrami and Ozawa equation shown that the better model for examination of this system.

1. Introduction

One of the most serious threats to the environment is plastics pollution and there is growing concern about the excess use of plastics, particularly in packaging. Almost 200 million tons of plastics are produced each year and within a short period of time nearly half of them are disposed to the environment [1–3].

Businesses and governments need to take responsibility for new ways to design, recover and dispose of plastics. Synthesis of biodegradable polymers has received considerable attraction in the recent years as an effective way to help reduce environmental pollution in the world. Applications of biodegradable polymers include packaging materials, bottles, medical implants, bone fixation, fabrics, drug delivery systems and agricultural mulch films [4]. Aliphatic polyesters are considered to be the most economically competitive of the biodegradable polymers [5].

During the last years, polymer-based nanocomposites containing silica nanoparticles (SiO_2) were successfully prepared and studied [6]. The amorphous SiO_2 nanoparticles were used as effective reinforcement filler in many polymer-based nanocomposites [6, 7]. Due to their extremely high surface area per unit weights, fumed silica particles with a particle size of about 15 nm exhibit a very high surface energy [8].

It is well known that the hydrophilic silica nanoparticles act as nucleating agent and addition of nanoparticles decreased the crystallization temperature of the polymers [9].

2. Experimental procedure

2.1. Materials

Adipic acid (99%) and ethylene glycol (98%) were purchased Merck Chemical Co. Fumed silica nanoparticle, SiO_2, used for preparation of the nanocomposites, were supplied by Degussa AG (Hanau, Germany) under the trade name AEROSIL® 200, having a specific surface area 200 m^2/g (>99.8% SiO_2) and average primary particle size 12 nm. Para-toluene sulphonic acid (PTSA) and zinc acetate dihydrate catalyst of analytical grade were purchased from Aldrich Chemical Co. All the other materials and solvents which were used for the analytical methods were of analytical grade.

2.2. Preparation of nanocomposite

PEAd/SiO_2 nanocomposites were prepared by in situ polymerization from the direct esterification of ethylene glycol with succinic acid in the presence of 3%wt. of SiO_2 nanoparticle in two steps:

First Step (Esterification): The amount of catalyst needed (1.8×10^{-3} mol of para toluenesulphonic acid per mol of acid) was added to a glass reactor containing a mixtures of adipic acid and ethylene glycol (mole ratio = 1/1.1). In this step, the mixture was heated at 170±3 ºC, under a low vacuum (60 kPa) and vigorously stirred. Vacuum is applied to facilitate removal of the produced water as the reaction proceeds. In the esterification step, at least 92% of theoretical water was removed from the reaction mixture by distillation and collected in a graduated cylinder.

Second Step (Polycondensation): The temperature was maintained at 185±3 ºC under high vacuum conditions (25 Pa), while zinc acetate dihydrate catalyst of the same above quantity was added. This step seems to be completed in 120 min for preparing of PEAd. The PEAd/SiO_2 nanocomposites were prepared via the in situ technique [10]. Finally, the products were ground in grind-mill, washed with methanol, and dried in vacuum at 50 °C for 24 h.

2.3. Charactrization of nanocomposite

Observation of dispersion SiO_2 nanoparticles in matrix of PEAd polymer carry out by scanning electron microscopy (SEM) images on a Philips XL-30ESEM equipped with an X-ray energy dispersive detector.

The kinetics of isothermal crystallization of pure PEAd and PEAd/SiO_2 nanocomposite samples were investigated by a Perkin Elmer, Pyris Diamond DSC. All measurements were carried out in nitrogen atmosphere. Function of the system at low temperatures (down to −65 ºC) was achieved using a Perkin Elmer Intracooler 2P cooling accessory.

The crystalline structure of the PEAd/SiO_2 nanocomposites was investigated by WAXD, using a Philips Pro Expert diffractometer with nickel filtered CuK_α radiation (λ = 0.154 nm) operated at a voltage of 3 kV, 5 mA current, 4°/ min scanning speed and 5°-55° (2θ) range.

3. Results and discussion

3.1. Characrerization of samples

Wide-angle X-ray diffraction (WAXD) patterns of the nanocomposites were also recorded. The results of WAXD analysis of pure PEAd and PEAd/SiO_2 nanocomposite containing 3% SiO_2 are shown in Fig. 1. α-Crystal type of PEAd and the PEAd/SiO_2 nanocomposite can be observed in the WAXD pattern. Although, the crystal type did not change after the incorporation of the SiO_2 nanoparticles in the PEAd matrix, a slightly increased intensity of the crystalline peak is shown in the patterns of pure PEAd, compared to the PEAd/SiO_2 nanocomposite. Based on the obtained WAXD result, it can be concluded that the PEAd/SiO_2 nanocomposite have a higher crystallinity. The spreading of the SiO_2 nanoparticles in pure PEAd is shown in Fig. 2. From the SEM microphotograph of the PEAd/SiO_2 3% nanocomposite, it can be seen that SiO_2 have a satisfactory dispersion in pure PEAd matrix.

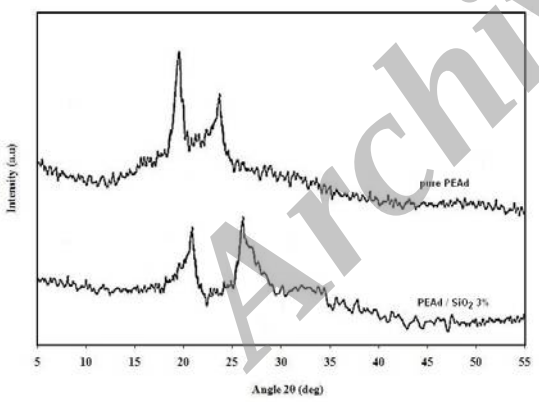

Fig. 1. WAXD patterns of samples at room temperature for pure PEAd and respective PEAd/SiO_2 nanocopmosite

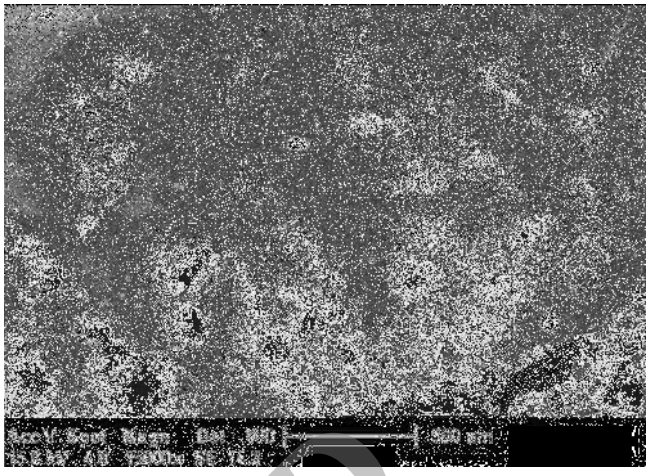

Fig.2. SEM microphotograph of (a) PEAd/SiO_2 3 wt.-% nanocomposite, appearing the dispersion of silica nanoparticles

3.2. Crystallization behavior of PEAd and PEAd/SiO_2 nanocomposite

The Crystallization behavior of the prepared PEAd and PEAd/SiO_2 nanocomposite has been studied by means of DSC. The DSC thermograms of the PEAd and PEAd/SiO_2 nanocomposite samples at various cooling rates are presented in Figs. 3 and 4. The peak temperature (*T*p) as a function of crystallization temperature can be obtained for describing the non-isothermal crystallization behavior of PEAd and PEAd/SiO_2 nanocomposite. According to this figure, It is clearly seen that *T*p shifts, as expected, to lower temperature with increasing cooling rate for pure PEAd and PEAd/SiO_2 nanocomposite. This indicates that lower crystallization time periods will affect the polymer's crystallization as increasing cooling rate. Therefore, in a fast cooling process, the motion of PEAd molecules cannot follow the cooling temperature. As shown in the DSC thermograms, for the small difference of scanning rate, i.e 5, 10, 15, 20 °C min^{-1}, the difference in T_p is not as much as excepted. Furthermore, for a given cooling rate, *T*p of PEAd/

SiO_2 nanocomposite is higher than that of pure PEAd as presented in Table 1. This can be concluded that SiO_2 nanoparticles have a heterogeneous nucleation effect on PEAd macromolecule segments.

3.3. Non-isothermal crystallization kinetics of PEAd and PEAd/SiO_2

For the prepared PEAd and PEAd/ SiO_2 3%wt., the crystallinity degree (X_c) can be determined from the enthalpy evolved during crystallization using the following equation:

$$X_c(T)=\frac{\int_{T_0}^{T}(dH_c/dT)dT}{(1-\chi)\int_{T_0}^{T_\infty}(dH_c/dT)dT}=\frac{A_0}{(1-\chi)A_\infty} \quad (1)$$

where T_0 and T_∞ are the initial and final crystallization temperatures, A_0 and A_∞ are areas under the normalized DSC curves and χ is the weight fraction of the filler in the nanocomposite.

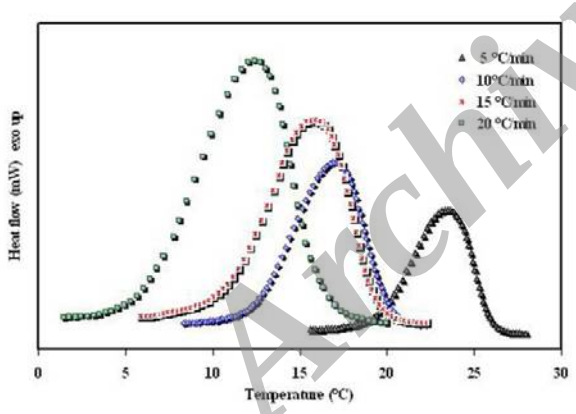

Fig. 3. DSC thermograms of non-isothermal crystallization for pure PEAd at different cooling rates.

Relative crystallinity as a function of temperature for pure PEA/SiO2 nanocomposite during non-isothermal crystallization is shown in Figs. 5 and 6. According to these figures, it can be seen that the curves have similar sigmoidal forms. The curvature of the upper parts of all the curves can be attributed to spherulite impingement in the later stages of crystallization.

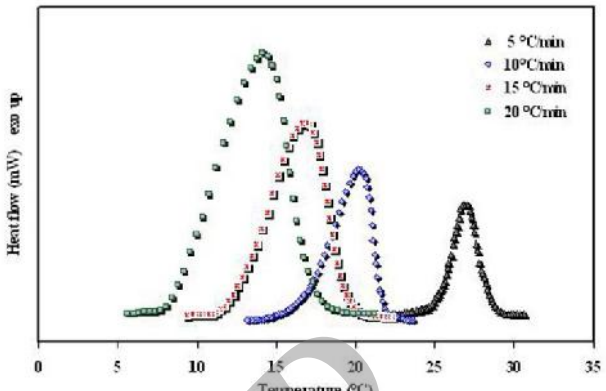

Fig. 4. DSC thermograms of non-isothermal crystallization for PEAd/SiO_2 3%wt. nanocomposite at different cooling rates.

The relationship between crystallization temperature and time during the non-isothermal crystallization process is given by the following form:

$$t=\frac{T_0-T}{\alpha} \quad (2)$$

where t is the crystallization time, T_0 is the temperature at which crystallization begins (t = 0), T is the crystallization temperature, and α is the cooling rate.

Table 1. DSC results for the polyesters and respective nanocomposites

Samples	Cooling Rate (°C/min)	T_p (°C)	ΔH_c ($J.g^{-1}$)	$t_{1/2}$ (min)	X_c (%)
Pure PEAd	5.0	23.5	57.1	0.92	40.8
	10	17.2	56.1	0.50	40.1
	15	16.9	54.9	0.43	39.2
	20	12.4	53.5	0.38	38.2
PEAd/SiO_2 3%	5.0	23.6	52.2	0.71	38.0
	10	18.6	51.9	0.36	37.8
	15	14.9	51.5	0.35	37.5
	20	13.8	51.2	0.34	37.3

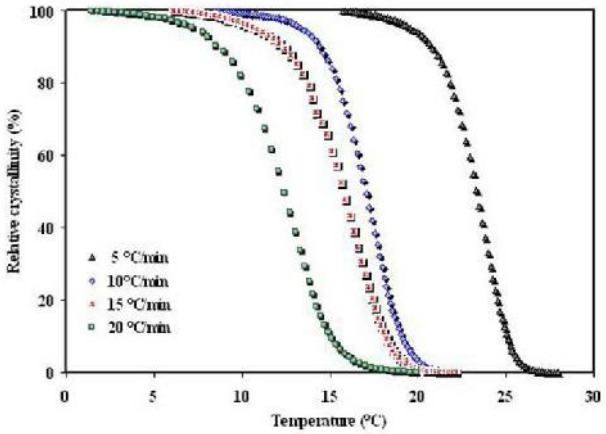

Fig. 5. Plots of relative crystallinity as a function of temperature for pure PEA during non-isothermal crystallization

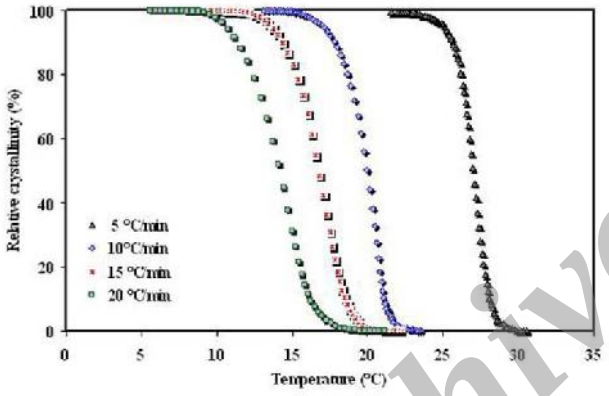

Fig. 6. Plots of relative crystallinity as a function of temperature for pure PEA/SiO_2 nanocomposite during non-isothermal crystallization

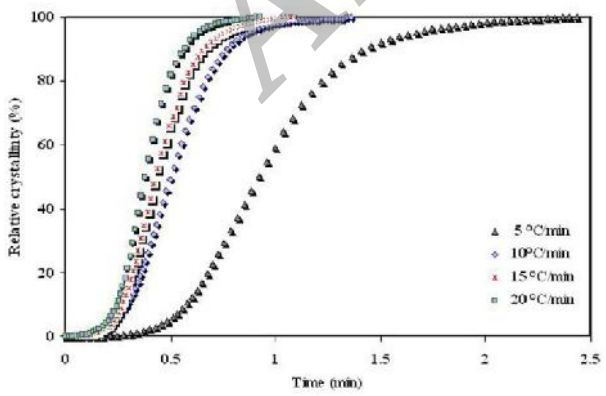

Fig. 7. Plots of relative crystallinity as a function of time for pure PEA during non-isothermal crystallization

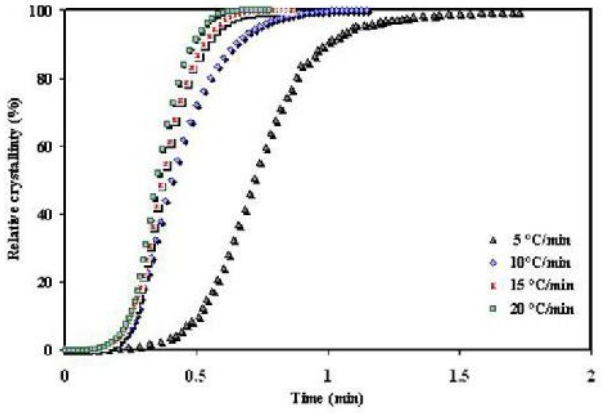

Fig. 8. Plots of relative crystallinity as a function of time for pure PEA/SiO_2 nanocomposite during non-isothermal crystallization

According to Eq. (2), the value of T on the X-axis in Figs. 5 and 6 can be transformed into the crystallization time t as shown in Figs. 7 and 8.

The polymer and nanocomposite non-isothermal crystallization can be described by the Avrami equation. which can write in the following form [11, 12]:

$$1 - X_c(t) = \exp\left(-Z_t t^n\right) \quad (3)$$

where the X_c *(t)* is the relative crystallinity at the crystallization time t. The n is Avrami exponent. The Z_t is the rate constant for crystallization. The double logarithm of the Eq. 3 gives the following relationships:

$$\log\left[-\ln\left(1 - X_c(t)\right)\right] = n \log t + \log Z_t \quad (4)$$

plotting $\log(-\ln(1 - X_c(t)))$ vs. $\log t$ for each cooling rate, gives a straight line which shown in Fig. 9 and 10 thus two adjustable parameters, n and Z_t, can be estimated from slope and intercept respectively and these values are listed in Table 2. It is well known that the parameter of Avrami exponent n describes the growing mechanism and geometry of crystallization, and the parameter Z_t describes the growth rate under the non-isothermal crystallization process.

Table 2. Non-isothermal crystallization kinetic parameters based on Avrami method

Samples	Cooling Rate (°C/min)	n	Z_t
Pure PEA	5.0	3.96	0.0139
	10	3.18	0.7641
	15	3.83	1.2020
	20	3.63	1.3144
PEA/SiO_2 2%	5.0	4.58	0.471
	10	3.98	1.4142
	15	4.36	1.6370
	20	5.04	2.1192

Although, the physical meanings of Z_t and n cannot be related to the non-isothermal case in a simple way, their use supplies further insight into the kinetics of non-isothermal crystallization. Taking the non-isothermal characteristics of the process exanimate, the parameter for the value of the crystallization rate, Z_t; should be corrected because the temperature was constantly changing during the process.

As a result of Table 2, the Avrami exponent n of pure PEAd ranged from 3.18 to 3.96 depending on the cooling rate, which indicated that the spherulite growth occurred with homogeneous nucleation.

The Avrami exponents n for silica nanoparticle-filled PEAd composites were greater than that for pure PEAd at the same cooling rate, indicating that the SiO_2 nanoparticles acted as heterogeneous nuclei for the initial nucleation. Hence, the type of nucleation and the geometry of crystal growth of PEAd were significantly changed by the presence of the silica nanoparticles.

The alternative approach to depict the crystallization mechanism of polymers under non-isothermal condition is the Ozawa equation [13], as followed:

$$1 - X(T) = \exp\left(-\frac{K(T)}{\alpha^m}\right) \quad (5)$$

$$\log\left[-\ln(1 - X(T))\right] = \log K(T) - m\log\alpha \quad (6)$$

where $X(T)$ is the relative degree of crystallization at temperature T, $K(T)$ is a cooling function depending on the overall crystallization rate, and m is the Ozawa exponent depending on the dimension of crystal growth. Correspondingly, if the Ozawa model can correct describe the crystallization behavior of polymer, then a plot of $\log\left[-\ln(1 - X(T))\right]$ against $\log\alpha$ will give a straight line, and the Ozawa exponent m and the $K(T)$ value can be also derived from the slope and the intercept, respectively.

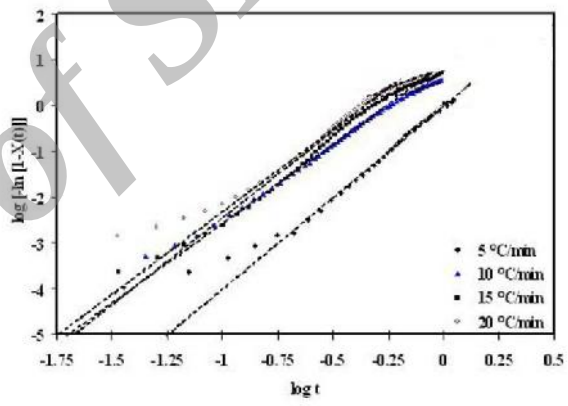

Fig. 9. Avrami curves of pure PEAd during non-isothermal crystallization

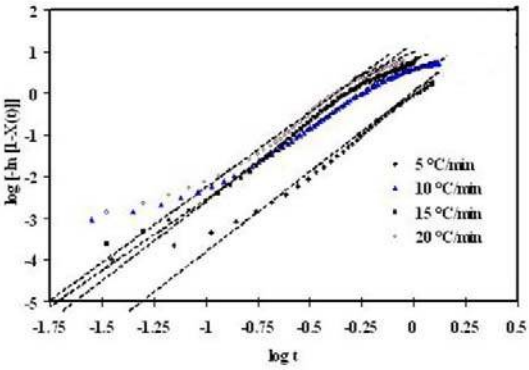

Fig. 10. Avrami curves of PEAd /SiO_2 nanocomposite during non-isothermal crystallization

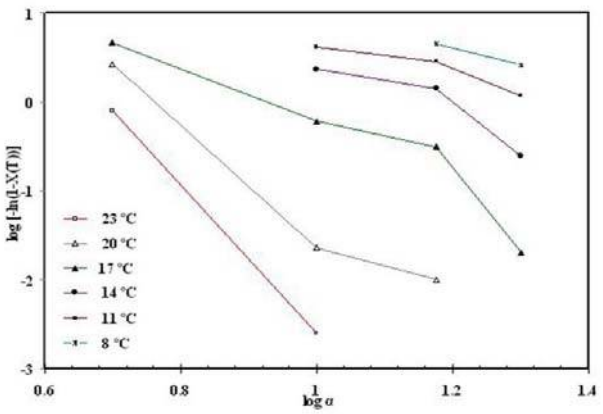

Fig. 11. Ozawa curves of pure PEAd during non-isothermal crystallization.

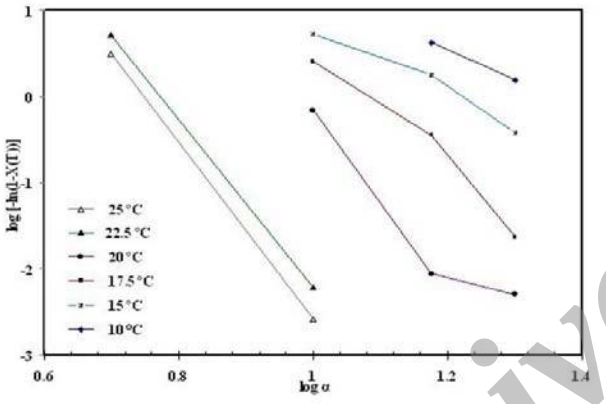

Fig. 12. Ozawa curves of PEAd /SiO_2 nanocomposite during non-isothermal crystallization

As shown in Fig. 11 and 12, the crystallization behaviors of the pure PEAd and the nanoparticle-filled PEAd composites are not accurately fitted to the Ozawa equation because of the curvatures in the plots. It is well known that the Ozawa model is based on the quasi-isothermal crystallization. Under non-isothermal crystallization, the crystallization rate is no long constant but a function of both time and cooling rate. Accordingly, in Ozawa analysis, both time and cooling rate could be reliable for the experimental data differences, indicating the varying physical states of the system. Therefore, these differences did not be taken into account in the Ozawa model. At a given crystallization temperature but under different cooling rate, the slow cooling could be just at the latest stage of crystallization, on the contrary, it is could be just at the initial stage for the high crystallization rate. Moreover, the slow secondary crystallization was not considered, and this neglect could lower the measured value of the Ozawa exponent. The other disregarded factor in the Ozawa model is the folded chain length of the polymer chain. It is well known that the folded chain length is a function of the crystallization temperature, suggesting that the different folded chain lengths should result under dynamic crystallization [14, 15].

Liu et al. [16] proposed a different kinetic equation by combining the Ozawa and Avrami equations. As the degree of crystallinity was related to the cooling rate and the crystallization time t (or temperature T), the relation between α and t could be defined for a given degree of crystallinity. Consequently, a new kinetic equation for nonisothermal crystallization was derived by combining Eqs. (4) and (6):

$$\log Z_t + n\log t = \log K(T) - m\log\alpha \quad (7)$$

$$\log\alpha = \log F(T) - b\log t \quad (8)$$

where the parameter $F(T)=[K(T)/Z_t]^{1/m}$; the Avrami exponent n is calculated using Ozawa's method, and b is the ratio between the Avrami and Ozawa exponents, i.e. $b= n/m$. $F(T)$ indicate the value of the cooling rate chosen at unit crystallization time, when the system has a defined degree of crystallinity. It can be seen that $F(T)$ has a specific physical and practical meaning. In accordance with Eq. (8), at a given degree of crystallinity the plot of log α against log t will give a straight line with an intercept of log $F(T)$ and a slope of $-b$: As shown in Figs. 12 and 13, plotting

log α against log t gave a linear relationship at a given degree of crystallinity, and the values of log $F(T)$ and b are listed in Table 3. The log $F(T)$ values increased with the relative degree of crystallinity, and b ranged from 1.20 to 1.53 for pure PEAd, and from 1.57 to 1.81 for nanocomposites. Therefore these equations successfully describe the non-isothermal crystallization process of PEAd and PEAd/SiO_2 nanocomposite.

Table 3. Activation energies and non-isothermal crystallization kinetic parameters based on Mo's equation

Samples	$X(T)$ (%)	log $F(T)$	b	E_a (KJ/mol)
Pure PEAd	15	0.4447	1.20	100.88
	30	0.5212	1.53	
	45	0.6225	1.49	
	60	0.7001	1.45	
	75	0.8050	1.33	
	90	0.9285	1.46	
PEA/SiO_2 3%	15	0.2560	1.64	85.22
	30	0.3861	1.57	
	45	0.4333	1.66	
	60	0.4977	1.69	
	75	0.5543	1.81	
	90	0.6786	1.75	

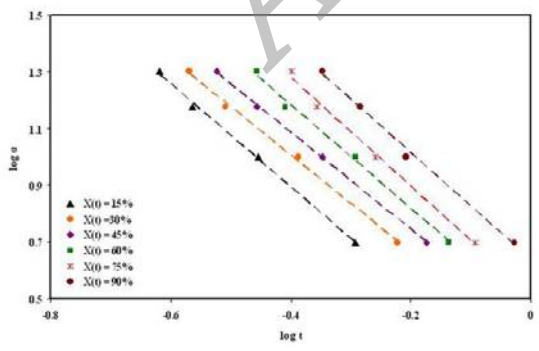

Fig. 12. The curves of log α versus log t for pure PEA base on combined Avrami and Ozawa equations at different relative degrees of crystallinity

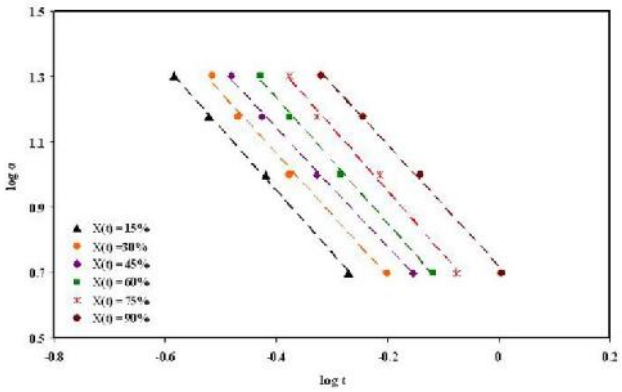

Fig. 13.The curves of log α versus log t for PEAd /SiO_2 nanocomposite base on combined Avrami and Ozawa equations at different relative degrees of crystallinity

3.3. Activation energy for non-isothermal crystallization

The activation energy for non-isothermal crystallization can be obtained from the combination of cooling rate and crystallization peak temperature, and Kissinger [17] proposed a method for calculating the activation energy for non-isothermal crystallization as explain:

$$\frac{\left[\ln\left(\alpha/T_p^2\right)\right]}{d\left(1/T_p\right)} = -\frac{E_a}{R} \qquad (9)$$

where R is the universal gas constant; Tp is the crystallization peak temperature; α is the cooling rate, and E_a is the crystallization activation energy. The activation energies of the non-isothermal crystallization for pure PEAd and the PEAd/ SiO_2 nanocomposites were obtained from the slope of the plot of $\ln\left(\alpha/T_p^2\right)$ versus $\left(1/T_p\right)$, according to Eq. (9), and the results are shown in Table 3. The activation energy of crystallization for PEAd/ SiO_2 nanocomposite was lower than that of pure PEAd. The variation in the activation energy for non-isothermal crystallization of PEAd/SiO_2 nanocomposites may be explained by changes in the crystallization mechanism and the free energy of nucleation with the degree of supercooling.

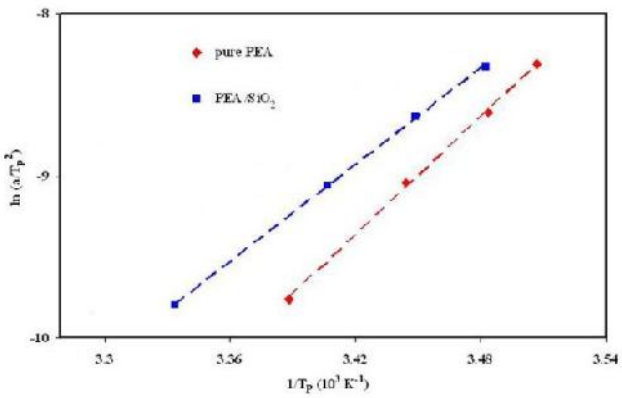

Fig. 14. Crystallization activation energies of selected samples

For PEAd/ SiO_2 nanocomposite system, the lower activation energy was related to that SiO_2 nanoparticles act as nucleating agents and may accelerate the non-isothermal crystallization of PEAd/ SiO_2 nanocomposite, which was confirmed by the kinetic parameters determined for nonisothermal crystallization and crystallization half-time.

4. Conclusion

The non-isothermal crystallization kinetics of biodegradable poly(ethylene adipate), PEAd and PEAd/SiO_2 3% nanocomposite were investigated by DSC. The results showed that the presence of SiO_2 nanoparticle promoted the nucleation.

In non-isothermal crystallization kinetics, the Ozawa model was inapplicable to describe the crystallization of the synthesized polyesters and nanocomposites, while the Avrami model and Mo's model were found to be suitable to explain the crystallization kinetics of these systems. The crystallization activation energies of the SiO_2 nanoparticle-filled polyesters composites are lower than that of the neat polyesters, reflecting the much lower energy barrier for the rapid heterogeneous nucleation.

References

[1] G.Z. Papageorgioua, D.N. Bikiaris, D.S. Achiliasa, E. Papastergiadisb, A. Docoslis Thermchim. Acta. 515 (2011) 13–23.

[2] L.Yu, K. Dean, L. Lin. Prog. Polym. Sci. 31 (2006) 576–602.

[3] M. Amirian, A. Nabipour Chakoli, W.Cai, J.H. Sui, Iran. Polym. J. 21 (2012) 165-174.

[4] A. Kumari, S.K. Yadav, S.C. Yadav, Coll. Surf. B: Biointerfaces 75 (2010) 1-18.

[5] V. Tserki, P. Matzinos, E. Pavlidou, D. Vachliotis, C.Panayiotou, Polym. Deg. and Stab. 91(2006) 367–376.

[6] Y. Peneva, L. Minkova, Polym. Test. 25 (2006) 366–376.

[7] D.S. Achilias, D.N. Bikiaris, E. Papastergiadis, D. Giliopoulos, G.Z. Papageorgiou, Macromol Chem Phys 211 (2010) 66–79.

[8] R.C. Rowe, P.J. Sheskey, M.E. Quinn, editors. Handbook of Pharmaceutical Excipients. 6th ed. Pharmaceutical Press and American Pharmacists Association (2009).

[9] X. Wen, Y. Lin, C. Han, K. Zhang, X. Ran, Y. Li, L. Dong. J. App. Polym. Sci. 114(2009) 3379-3388.

[10] M.Mohsen-nia, M.R.Memarzadeh, Polym. Bull. 70 (2013) 2471-2491.

[11] M. Avrami. J Chem Phys 7 (1939) 1103–1112.

[12] M. Avrami. J Chem Phys 8 (1940) 212–224.

[13] T. Ozawa, Polymer 12 (1971) 150-158.

[14] J.Y. Kim, H.S. Park, S.H. Kim, Polymer 47 (2006) 1379–1389.

[15] M.C. Kuo, J.C. Huanga, M. Chena, Mat. Chem. and Phys. 99 (2006) 258–268.

[16] T. Liu, Z. Mo, S. Wang, H. Zhang, Polym. Eng. Sci. 37 (1997) 568-575.

[17] H.E. Kissinger, J. Res. Natl. Stand. 57 (1956) 217- 221.